[12]Dolling, D. S., and Murphy, M. T., "Unsteadiness of the Separation Shock Wave Structure in a Supersonic Compression Ramp Flowfield," *AIAA Journal*, Vol. 21, No. 12, 1983, pp. 1628–1634.

Active Control of Boundary-Layer Instabilities: Use of Sensors and Spectral Controller

R. D. Joslin,* R. A. Nicolaides,† G. Erlebacher,‡
M. Y. Hussaini,§ and M. D. Gunzburger¶
NASA Langley Research Center,
Hampton, Virginia 23681-0001

Introduction

THIS second study focuses on the suppression of instability growth using an automated active-control technique. This automated approach is the next logical step based on previous experimental and computational studies reviewed by Joslin et al.[1] and Thomas,[2] in which the control was in the form of wave cancellation. The wave-cancellation method assumes that a wavelike disturbance can be linearly canceled by introducing another wave that has a similar amplitude but that differs in phase. Both experimental and computational results have demonstrated that two-dimensional Tollmien–Schlichting (TS) waves can be superposed upon two-dimensional waves in such a way as to reduce the amplitudes in the original waves under the presumption of wave cancellation. Joslin et al.[1] have definitively shown that flow control by wave cancellation is the mechanism for the observed phenomena. Three simulations were performed in their computational study to demonstrate the wave-cancellation concept. The first simulation obtained the evolution of a two-dimensional instability generated by periodic suction and blowing forcing, the second simulation yielded an instability caused by a suction and blowing actuator in the absence of and downstream of the forcing used in the first simulation, and the third simulation computed the evolution of a disturbance resulting from both forcing and actuator suction and blowing (wave-cancellation test case). Joslin et al.[1] showed that the superposition of the first and second simulation results exactly matched the wave-cancellation simulation results.

Based on the wave-cancellation assumption, the evolution and automated control of spatially growing two-dimensional disturbances in a flat-plate boundary layer are computed. Although the present active-control approach is demonstrated here for a two-dimensional instability test case, the ultimate goal of this line of research is to introduce automated control to external flow over an actual aircraft or to any flow that has instabilities that require suppression.

The nonlinear computations consist of the integration of the sensors, actuators, and controller as follows: the sensors will record the unsteady pressure or shear on the wall; the spectral analyzer (controller) will analyze the sensor data and prescribe a rational output signal; the actuator will use this output signal to control the disturbance growth and stabilize the instabilities within the laminar boundary layer. This scenario is shown in Fig. 1. Although a closed-loop feedback system could be implemented (using an additional sensor downstream of the actuator) to fully automate the control and to lead to an exact cancellation of the instability, the feedback will not be introduced here due to the added computational expense of the iterative procedure.

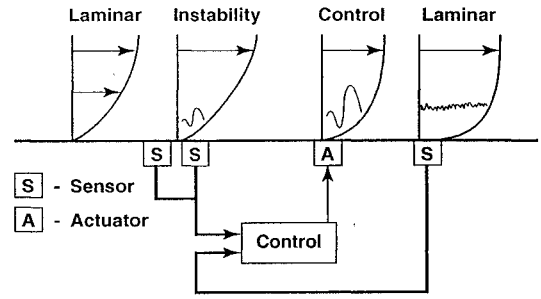

Fig. 1 Schematic of active control with wave cancellation.

Numerical Techniques

The nonlinear, unsteady Navier–Stokes equations are solved by direct numerical simulation (DNS) of disturbances, which evolve spatially within the boundary layer. The spatial DNS[3,4] approach involves spectral and high-order finite difference methods and a three-stage Runge–Kutta method[5] for time advancement. The influence-matrix technique is employed to solve the resulting pressure equation.[6,7] Disturbances are forced into the boundary layer by unsteady suction and blowing through a slot in the wall. At the outflow boundary, the buffer-domain technique of Streett and Macaraeg[8] is used.

The equations are nondimensionalized with the freestream velocity U_∞, the kinematic viscosity ν, and the inflow displacement thickness δ_0^*. The Reynolds number becomes $R = U_\infty \delta_0^*/\nu$, and the frequency is $\omega = \omega^* \delta_0^*/U_\infty$.

Control Method

Here, the term "controller" refers to the logic that is used to translate sensor-supplied data into a response for the actuator, based on some control law. For the present study, a spectral controller requires a knowledge of the distribution of energy over frequencies and spatial wave numbers. For this automated controller system, a minimum of two sensors must be used to record either the unsteady pressure or unsteady shear at the wall. By using Fourier theory, this unsteady data can be transformed via

$$f(\omega) = \int_{-\infty}^{\infty} f(t) e^{-i\omega t}\, dt \tag{1}$$

where $f(t)$ is the signal and ω is the frequency. This transform yields an energy spectrum that indicates which frequencies exist in the signal and how much relative energy each frequency contains.

The largest Fourier coefficient indicates the frequency that will be used to control the instability, although the largest growth rate can be used instead of largest coefficient. The information from the two sensors is used to obtain estimates of both spatial growth rates and phase via the relation

$$\alpha = \frac{1}{A}\frac{dA}{dx} \tag{2}$$

This temporal and spatial information is then substituted into the assumed control law, or wall-normal velocity boundary condition,

$$v_s(x, t) = v_w \times p_w^1 \exp\left[i(\omega + \phi_t)t + \alpha x_s\right] + \text{c.c.} \tag{3}$$

where p_w^1 is the complex pressure (or shear) for the dominant frequency mode (or largest growth-rate mode) at the first sensor, ω is the dominant mode determined from Eq. (1), ϕ_t is the phase

Received Nov. 26, 1994; revision received Jan. 31, 1995; accepted for publication Jan. 31, 1995.

*Research Engineer, Fluid Mechanics and Acoustics Division. Member AIAA.

†Consultant, Institute for Computer Applications in Science and Engineering; currently Professor, Department of Mathematics, Carnegie Mellon University, Pittsburgh, PA 15213.

‡Research Fellow, Institute for Computer Applications in Science and Engineering. Member AIAA.

§Director, Institute for Computer Applications in Science and Engineering. Member AIAA.

¶Consultant, Institute for Computer Applications in Science and Engineering; currently Professor, Department of Mathematics, Virginia Polytechnic Institute and State University, Blacksburg, VA 24061.

information, t is the time, α is the growth-rate and wave number information calculated from Eq. (2), and x_s is the distance between the first sensor and the actuator. Because the sensor information can be used only to approximate the actuator amplitude and temporal phase, v_w and ϕ_t are parameters that must be optimized to obtain exact wave cancellation. This may be accomplished through, for example, a gradient descent algorithm. (Here, no attempt was made to demonstrate exact wave cancellation.)

This control law is used only for this feasibility study. Aspects of formal optimal-control theory and artificial neural-network algorithms are currently being tested by the authors for use in a subsequent study.

Numerical Experiments

For this study, we are not concerned with the method by which disturbances are ingested into the boundary layer; the underlying assumption here is that natural transition involves some dominant disturbances that can be characterized by waves. In a subsequent study, we will explore controlling transition consisting of either random unsteady or three-dimensional nonlinear and arbitrary instabilities. Here, the instabilities are assumed to be characterizable by discrete frequencies within the spectrum.

For the computations, the grid has 661 streamwise and 61 wall-normal points. The far-field boundary is located $75\delta_0^*$ from the wall, and the streamwise distance is $308\delta_0^*$ from the inflow, which is equal to approximately 11 TS wavelengths. The disturbance frequency is $Fr = \omega/R \times 10^6 = 86$, and the Reynolds number is $R = 900$ at the inflow. (The streamwise range of the computations and the relative sensor and actuator are located within the unstable region of the linear stability neutral curve.) A time-step size of 320 steps per period is chosen for the three-stage Runge–Kutta method. To complete a two-dimensional, simulation, 0.9 h on the Cray Y-MP are required with a single processor. (Refer to Ref. 3 for details on accuracy issues with grid refinement.)

For this study, the disturbance forcing slot has a length $5.13\delta_0^*$ and is centered $23.10\delta_0^*$ downstream of the computational inflow boundary. The first sensor is located $57.88\delta_0^*$ downstream of the inflow, and the second sensor is located $2.33\delta_0^*$ downstream of the first sensor. The actuator has a slot length $4.67\delta_0^*$ and is located $77.94\delta_0^*$ downstream of the inflow boundary. These separation distances were chosen arbitrarily for this demonstration. Ideally, the forcing, sensors, and actuator should have a minimal separation distance to improve the accuracy of the sensor information provided to the actuator.

A small-amplitude disturbance ($v_f = 0.01\%$) is forced at the inflow and controlled via the automated control law without feedback. Figure 2 shows the TS wave amplitudes with downstream distance for the present results compared with the control case ($v_w = 0.9v_f$; $\phi_t = 1.2\pi/\omega$) of Joslin et al.[1] and the uncontrolled wave. The

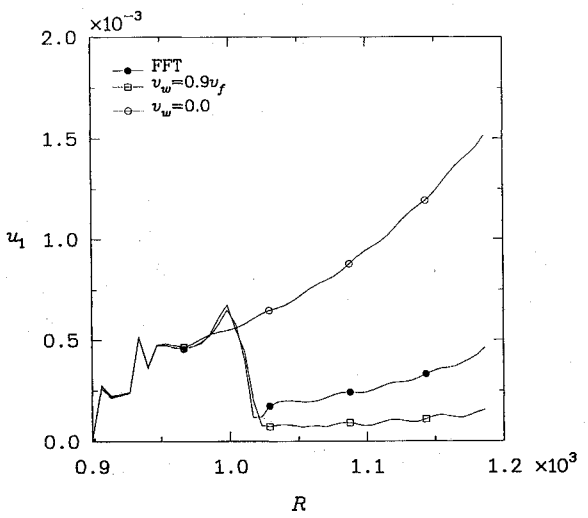

Fig. 2 Active control of small-amplitude TS waves in flat-plate boundary layer.

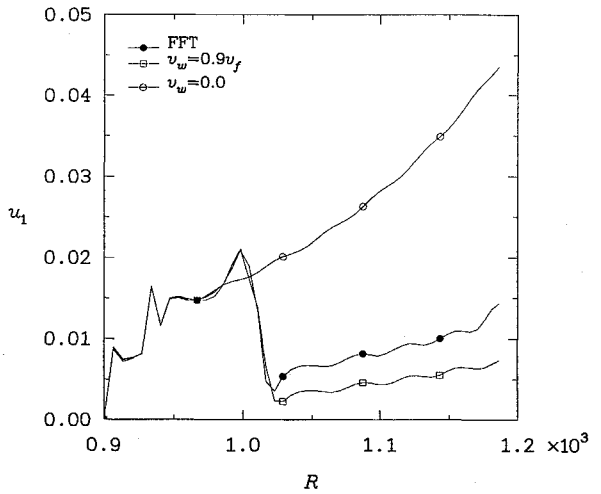

Fig. 3 Active control of large-amplitude TS waves in flat-plate boundary layer.

present results demonstrate that a measure of wave cancellation can be obtained from the automated system before initiating feedback; however, feedback is necessary to optimize the control amplitude and phase for exact cancellation of the disturbance.

Next, the evolution and control of a large-amplitude disturbance ($v_f = 3\%$) is studied. This large-amplitude case excites harmonics and a mean-flow distortion component with much smaller amplitudes than the fundamental-mode amplitude. Figure 3 shows comparisons for the control of the large-amplitude case. Again, the automated control can clearly obtain a degree of wave cancellation for large-amplitude instabilities without optimization and without causing the harmonics to prematurely grow. These test cases demonstrate that automated control can be effective with the presumption of discrete frequency instability waves.

Conclusions

Full Navier–Stokes simulations were conducted to determine the feasibility of automating the control of wave instabilities within a flat-plate boundary layer with sensors, actuators, and a spectral controller.

The results indicate that a measure of wave cancellation can be obtained for small- and large-amplitude instabilities without feedback; however, feedback is required to optimize the control amplitude and phase for exact wave cancellation.

This study is only the second in a series aimed at suppressing the instabilities that lead to transition within an otherwise laminar boundary layer with unsteady flow control. Follow-on research will focus on coupling optimal control theory with the Navier–Stokes equations to devise a control methodology without distinct control laws. This methodology focuses on the minimization of the wall shear at a prescribed region downstream of the actuator. This flow control could lead to suppression of arbitrary instabilities in a laminar boundary layer, drag reductions in a turbulent boundary layer, or enhanced lift by separation control.

Acknowledgment

This research was supported by NASA under Contract NAS1-10801 while the authors (except the first author) were in residence at the Institute for Computer Applications in Science and Engineering, NASA Langley Research Center, Hampton, Virginia.

References

[1]Joslin, R. D., Erlebacher, G., and Hussaini, M. Y., "Active Control of Instabilities in Laminar Boundary-Layer Flow. An Overview," *Journal of Fluids Engineering* (submitted for publication); see also Inst. of Computer Applications in Science and Engineering, ICASE Rept. 94–97, Hampton, VA, Dec. 1994.

[2]Thomas, A. S. W., "Active Wave Control of Boundary-Layer Transition," *Viscous Drag Reduction in Boundary Layers*, edited by D. M. Bushnell and J. N. Hefner, Vol. 123, Progress in Astronautics and Aeronautics, AIAA, Washington, DC, 1987, pp. 179–202.

[3]Joslin, R. D., Streett, C. L., and Chang, C.-L., "Validation of Three-Dimensional Incompressible Spatial Direct Numerical Simulation Code—A Comparison with Linear Stability and Parabolic Stability Equations Theories for Boundary-Layer Transition on a Flat Plate," NASA TP-3205, July 1992.

[4]Joslin, R. D., Streett, C. L., and Chang, C.-L., "Spatial DNS of Boundary-Layer Transition Mechanisms: Validation of PSE Theory," *Theoretical Computational Fluid Dynamics*, Vol. 4, No. 6, 1993, pp. 271–288.

[5]Williamson, J. H., "Low-Storage Runge–Kutta Schemes," *Journal of Computational Physics*, Vol. 35, No. 1, 1980, p. 48.

[6]Danabasoglu, G., Biringen, S., and Streett, C. L., "Spatial Simulation of Instability Control by Periodic Suction and Blowing," *Physics of Fluids*, Vol. 3, No. 9, 1991, pp. 2138–2147.

[7]Streett, C. L., and Hussaini, M. Y., "A Numerical Simulation of the Appearance of Chaos in Finite-Length Taylor-Couette Flow," *Applied Numerical Mathematics*, Vol. 7, No. 1, 1991, p. 41.

[8]Streett, C. L., and Macaraeg, M. G., "Spectral Multi-Domain for Large-Scale Fluid Dynamic Simulations," *Applied Numerical Mathematics*, Vol. 6, No. 1–2, 1989/1990, p. 123.

Application of Similarity in Hypersonic Transition Prediction

Alexander V. Fedorov* and Norman D. Malmuth†
Rockwell International Science Center, Thousand Oaks, California 91358

Introduction

PREDICTION of laminar-turbulent transition in hypersonic boundary layers is of critical importance for aircraft and missile design.[1] Although considerable effort has been invested in developing theoretical and computational methods to predict high Mach number transition, a strong need still exists for approaches suitable for rapid response design application. To fill this need, empirical criteria based on wind tunnel and flight experiments are currently the main workhorses in engineering practice. Much of the difficulty in constructing a rapid design oriented method is due to the unique features of the hypersonic stability and transition problem that include strong nonparallelism and shock effects. In spite of the success of e^N methods such as those in Ref. 2 below Mach 12, these aspects are significant at higher Mach numbers.

In this Note, similarity methods will be used to indicate a new, potentially useful procedure for preliminary design and fast tradeoff studies. These methods have the potential of dealing with some of these difficulties. The theoretical basis for the similarity method will be given and an application to hypersonic cones provided. Finally, possibilities for generalization of the method to more arbitrary shapes will be discussed.

Since the problem of disturbance evolution contains the large Mach and Reynolds number parameters, it is natural to use asymptotic methods in predictive models. Asymptotic theories for the vorticity mode, crossflow instability Gortler vortices, and the analysis of Ref. 3 are recent examples. Solutions from this class of asymptotic models are limited in their applicability because of the restrictive asymptotic limit processes used. Other asymptotic approximations provide more general applicability but are also more difficult to solve. Even without solution, however, such theories give important similarity groups, if appropriate normalizations and nondimensionalizations are used that reflect the salient phenomenological scales. These groups provide the basis for constructing similarity laws that can be useful not only for design of economical experiments but also for prediction as well.

Such a procedure will be used in this paper to investigate similitude of boundary-layer stability over nearly sharp, zero-incidence hypersonic cones. A similarity rule accounting for viscous and compressibility effects is derived without solving the initial boundary value problem. Predictions from the rule are compared with linear stability computations as well as (re-entry F) flight data obtained on slender cones.[4] It will be seen that this rule gives an extremely cost-effective and rapid extrapolation method of code or experimentally derived data to other conditions.

Similarity Analysis

The unsteady disturbance field in a three-dimensional hypersonic boundary layer will be considered with the following assumptions. 1) The fluid is a perfect gas with constant Prandtl number Pr and specific heat ratio γ. Denoting starred quantities as dimensional, the viscosity–temperature law is $\mu^* = \mu_0^* T^{*\omega}$. 2) The spatial scales of the disturbances are of the order of boundary-layer displacement thickness δ^*; the time scale is δ^*/U_e^*, where subscript e refers to the upper edge of the boundary layer. 3) Boundary-layer disturbances weakly interact with the external inviscid flow and shock wave.

In the hypersonic boundary layer, the pressure is of the order of that of the external inviscid flow, and the temperature is of the order of the stagnation temperature $T_s^* \sim (\gamma - 1)M_e^2 T_e^*$. This leads to asymptotic scaling for the flow variables within the boundary layer. The full Navier–Stokes equations written in terms of this scaling contain only the lumped parameter $R = \varepsilon^{1+\omega} Re$, where $\varepsilon \equiv 1/[(\gamma - 1)M_e^2] \ll 1$ and Re is the Reynolds number based on the displacement thickness, $Re = \delta^* U_e^* \rho_e^*/\mu_e^*$. The dependence on the similarity parameter R is valid for strong, moderate, and weak viscous-inviscid interaction regimes. However, δ^* and, as a result, the Reynolds number Re are sensitive to the interaction type. For example, the boundary layer on a flat plate has the displacement thickness $\delta^* \sim x^{*3/4}$ for strong interaction and $\delta^* \sim x^{*1/2}$ for a weak one.

Outside the boundary layer, the disturbances are assumed to vanish and weakly interact with the external inviscid flow. At the wall, the flow satisfies no-slip conditions, and temperature is assumed to be constant. The upstream and downstream conditions as well as initial conditions for the disturbances are also assumed to depend weakly on Mach and Reynolds number. These additional provisions preserve the applicability of the R similitude previously indicated. It is therefore clear that the similarity law

$$f = fn(R, \gamma, T_f, Pr) \tag{1}$$

holds, where f is any of the flow-dependent variables, T_f is the wall temperature ratio, and fn signifies a functional dependence that can be obtained from solution of the initial value problem.

This similarity can be extended to the linear stability problem if a typical eigenmode wavelength λ^* is of the order of the boundary-layer thickness. If small disturbances are assumed in the original form of the Navier–Stokes equations before the previously mentioned rescaling is used, the general linearized equations (LSE) for small fluctuations are obtained. Within the spatial and temporal scaling implied by the wavelength assumption, the equations for the fluctuations depend again only on the parameters γ, T_f, Pr, and R if further, their initial and boundary conditions are consistent with this assumption. Therefore, the fluctuations obey a similarity law such as Eq. (1).

As an example, consider the two-dimensional vorticity mode (second mode according to Mack's classification[5]) in the boundary layer on a flat plate or sharp cone. In this case, the span component of the wave vector $\beta = 0$ and the growth rate $\sigma = -\mathrm{Im}(\alpha)$ (where $\alpha =$ the complex eigenvalue). If the Prandtl number, specific heat ratio, and viscosity exponent parameters Pr, γ, and ω, as well as the wall temperature factor $T_f = T_w^*/T_{ad}^*$, are fixed, where T_w^* is the wall temperature, and T_{ad}^* is the adiabatic wall temperature, the maximum growth rate $\sigma_m(\Omega)$ ($\Omega = \Omega^* \delta^*/U_e^*$ the nondimensional frequency), is a function of Reynolds number Re and Mach number M_e.

In Fig. 1, calculations for σ_m from a linear stability code are shown as a function of the similarity parameter R at $M_e = 7$, 8, 10, 12, and

Received July 23, 1994; revision received Feb. 2, 1995; accepted for publication Feb. 2, 1995.

*Consultant; also Principal Researcher, Moscow Institute of Physics and Technology, 16 Gagarin Street, 140160 Zhukovsky, Russia.

†Project Manager, Computational Fluid Dynamics, 1049 Camino Dos Rios. Fellow AIAA.